1   **Rippling pattern of distortion product otoacoustic emissions evoked by high-frequency**

2   **primaries in guinea pigs**

3   George W.S. Burwood[a], Ian J. Russell, Andrei N. Lukashkin[b]

4   Sensory Neuroscience Research Group, School of Pharmacy and Biomolecular Sciences,

5   University of Brighton, Brighton, BN2 4GJ, UK

6   [a]Current address: Oregon Hearing Research Center, Oregon Health and Science University,

7   3181 SW Sam Jackson Park Rd, Portland, Oregon 97239, USA

8   **Short title:** High-frequency emissions in guinea pigs

9   **[b]Corresponding Author:**

10   Andrei N. Lukashkin

11   School of Pharmacy and Biomolecular Sciences

12   Huxley Building, University of Brighton

13   Lewes Road, Brighton, BN2 4GJ, UK

14   Tel: +44 1273 642103

15   E-mail: a.lukashkin@brighton.ac.uk

16

17

18

19

20

21 **ABSTRACT**

22 The origin of ripples in DPOAE amplitude which appear at specific DPOAE frequencies

23 during f_1 tone sweeps using fixed high frequency f_2 (>20kHz) in guinea pigs is investigated.

24 The peaks of the ripples, or local DPOAE amplitude maxima, are separated by approximately

25 half octave intervals and are accompanied by phase oscillations. The local maxima appear at

26 the same frequencies in DPOAEs of different order and velocity responses of the stapes and

27 do not shift with increasing levels of the primaries. A suppressor tone had little effect on the

28 frequencies of the maxima, but partially suppressed DPOAE amplitude when it was placed

29 close to the f_2 frequencies. These findings agree with earlier observations that the maxima

30 occur at the same DPOAE frequencies, which are independent of the f_2 and the primary ratio,

31 and thus are likely to be associated with DPOAE propagation mechanisms. Furthermore, the

32 separation of the local maxima by approximately half an octave may suggest that they are due

33 to interference of the travelling waves along the basilar membrane at the frequency of the

34 DPOAE. It is suggested that the rippling pattern appears because of interaction between

35 DPOAE reverse travelling waves with standing waves formed in the cochlea.

36

37

38

39

40

41

42

43

I. INTRODUCTION

The behaviour of the amplitude and phase of distortion product otoacoustic emissions (DPOAEs) generated by the cochlea during two-tone stimulation (Kemp, 1979) is complex. The DPOAE amplitude and phase behaviour depends on the animal species and the frequencies, levels, and separation of the primary tones (f_1 and f_2, $f_2 > f_1$). Many characteristics of DPOAEs and their generation mechanisms have been explored, including the existence of DPOAE fine structure, the non-monotonic behaviour of emissions as a function of frequency and level of the primaries, and band pass filtering produced as a function of primary frequency ratio (for review see Avan *et al*., 2013). However, a complete understanding of DPOAE generation and propagation is still lacking.

There is a general consensus that DPOAEs recorded in the ear canal are the vector sums of emissions generated by at least two sources (Brown *et al*., 1996; Shera and Guinan, 1999; Talmadge *et al*., 1999, Knight and Kemp, 2000; Kalluri and Shera, 2001). One source is the overlap between the two primary tones (Russell and Nilsen, 1997), where energy at the distortion frequencies is produced (Brown and Kemp, 1984) and elicits a travelling wave in the forward and reverse directions. The forward travelling wave peaks closer to the apex of the cochlea at the distortion characteristic frequency (CF) place, and is partially reflected back out of the cochlea, due to random mechanical irregularities along the organ of Corti (Kemp and Brown, 1983; Hilger *et al*., 1995; Zweig and Shera, 1995; Shera and Guinan, 1999; Konrad-Martin *et al*., 2001). The mixing of these two emissions, so called distortion-source and reflection-source emissions, has been shown to cause fine structure of DPOAE recorded in the ear canal (Heitmann *et al*., 1998; Talmadge *et al*., 1999). However, such mechanical irregularities putatively responsible for generation of reflection-source emission are less prominent in rodents (Kemp, 1986; Lonsbury-Martin *et al*., 1988; Shera and Guinan, 1999), and DPOAEs measured in rodent species do not display the rapidly changing fine

69 structure of human DPOAEs (Withnell *et al*., 2003). This observation has led to a debate as

70 to the mechanism behind the non-monotonic changes in DPOAE amplitudes during changes

71 of the primary frequencies in non-human mammal species (Lukashkin and Russell, 2001;

72 Withnell *et al*., 2003; Goodman *et al*., 2003; Lukashkin *et al*., 2007; de Boer *et al*., 2007).

73 The rippling of the DPOAE amplitude with distinct local maxima observed for specific

74 DPOAE frequencies when the primary frequency ratio f_2/f_1 is varied and f_2 is kept constant

75 have been described (Lukashkin *et al*., 2007). These local amplitude maxima appeared at

76 similar frequencies for moderate sound pressure levels across animals of the same species

77 and across different f_2 frequencies. Maxima at similar frequencies were also reported when

78 measuring higher order emissions ($3f_1$-$2f_2$ and $4f_1$-$3f_2$). The finding that the local amplitude

79 maxima were observed at the same DPOAE frequencies in emissions of different orders and,

80 hence, for different primary ratios indicates that these maxima may be related to the

81 propagation rather than the generation of DPOAEs. It was suggested (Lukashkin *et al*., 2007)

82 that this rippling pattern may be due to formation of standing waves in the cochlea (Kemp,

83 1979; Russell and Kössl, 1999; Goodman *et al*., 2003; Shera, 2003). Cochlear standing waves

84 may form during the DPOAE back propagation as a slow wave (Vetešník and Gummer,

85 2012), with the possibility that, in a variety of experimental paradigms, the formation of

86 standing waves can contribute to the non-monotonic behaviour of DPOAE amplitude.

87 In this paper we further investigate the rippling, non-monotonic behaviour of the distortion

88 product amplitude in acoustic responses of the cochlea and mechanical responses of the

89 stapes during variation of the primary frequency ratio and levels of the primary tones, and in

90 the presence of a suppressor tone. It is concluded that local DPOAE amplitude maxima are

91 due to formation of cochlear standing waves.

92 **II. METHODS**

A. Animal preparation

Data collected from 9 pigmented guinea pigs (male and female 172-393g) was used in this study. DPOAE data were collected from 4 animals and a further 5 animals were used for combined recording of DPOAE and mechanical responses of the stapes. All procedures involving animals were performed in accordance with UK Home Office regulations with approval from the University of Brighton Animal Welfare and Ethical Review Body. Guinea pigs were anaesthetised with the neurolept anaesthetic technique, (0.06 mg/kg body weight atropine sulphate s.c., 30mg/kg pentobarbital i.p., and 500 μl/kg Hypnorm i.m.). Additional injections of Hypnorm were given every 40 minutes at half of the initial dose. Additional doses of pentobarbital were administered as needed to maintain a non-reflexive state. The heart rate was monitored with a pair of skin electrodes placed on both sides of the thorax. The animals were tracheotomised and artificially ventilated, and their core temperature was maintained at 38ºC with a heating blanket and heated head holder. The middle ear cavity was opened to reveal the round window and the middle ear ossicles.

B. Sound stimulation and DPOAE recording

Sound was delivered to the tympanic membrane by a closed acoustic system comprising of two Bruel & Kjaer 4131 ½-inch speakers for delivering tones and a single Bruel & Kjaer 3133 ½ inch microphone for monitoring sound pressure. The sound system was coupled to the ear canal via 1 cm long, 4 cm diameter tubes to a conical speculum, the 1 mm diameter opening of which was placed about 1 mm from the tympanic membrane. The closed sound system was calibrated in situ for frequencies between 1 and 50 kHz. Known sound-pressure levels were expressed in dB SPL re: 2×10^{-5} Pa. All sound stimuli in this work were shaped with raised cosines of 0.5 ms in duration at the beginning and end of stimulation. White noise for acoustical calibration and tone sequences for auditory stimulation were synthesised by a

117   Data Translation 3010 board at a sampling rate of 250 kHz and delivered to the microphones

118   through low-pass filters (100 kHz cut-off frequency). Signals from the measuring amplifier

119   were digitized at 250 kHz using the same board and averaged in the time domain. Amplitudes

120   of the spectral maxima were obtained by performing an FFT on a time domain averaged

121   signal, 4096 points in length. The maximum level of system distortion measured with an

122   artificial ear cavity for the highest levels of primaries used in this study (L_1=70 dB SPL) was

123   70 dB below the primary level.

124   DPOAE ratio functions were recorded using f_1 sweeps with constant f_2. Levels of the

125   primaries, L_1 and L_2, were constant during each sweep with L_1=L_2+10 dB. For suppression

126   experiments, a calibrated 67 dB SPL suppressor tone was added using a Philips PM1593

127   programmable function generator, and ratio functions were recorded in the presence of

128   different suppressor frequencies. The simultaneous suppression paradigm was implemented.

129   The suppressor was presented over the duration of the primaries.

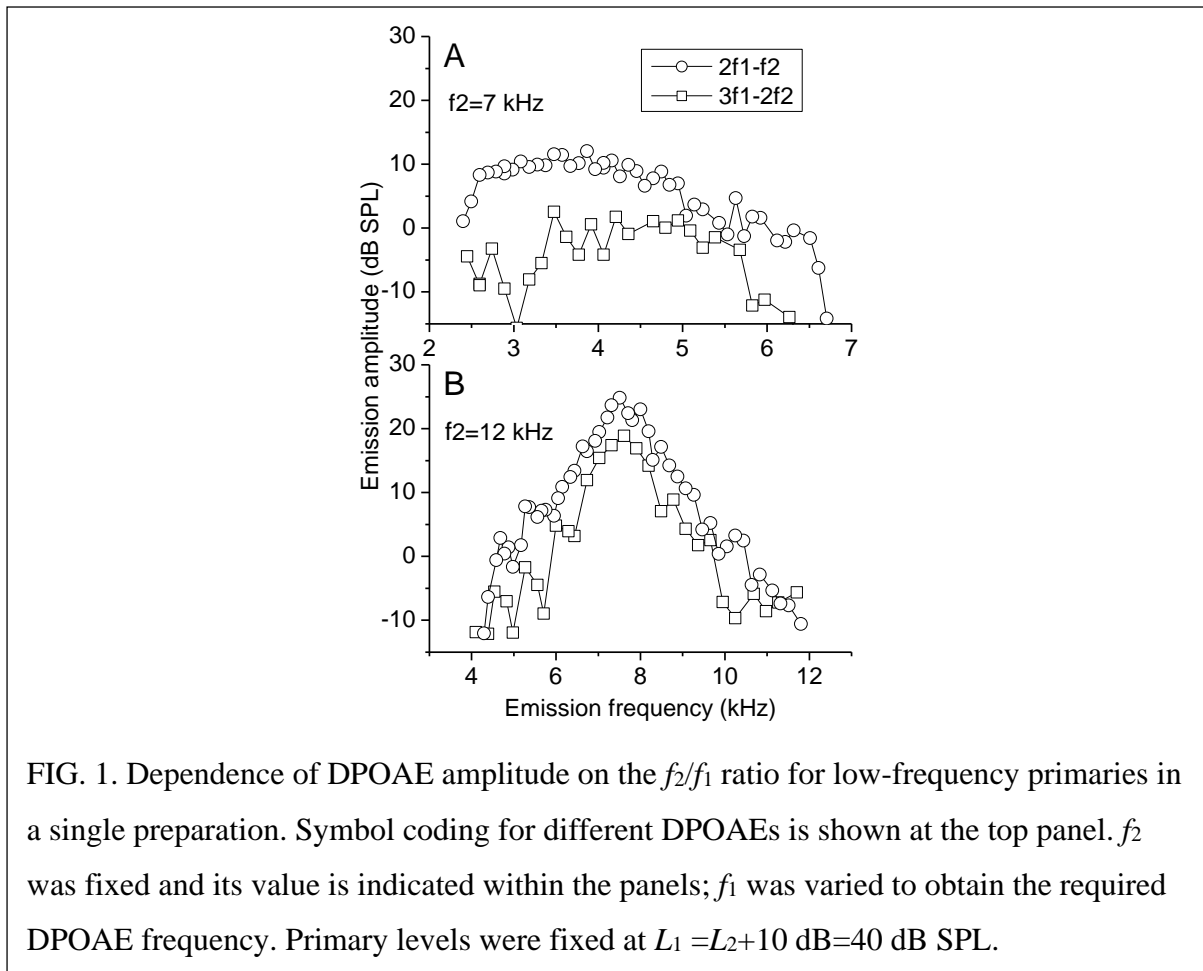130   **C. Recording of stapes vibrations**

131   Stapes vibrations were recorded using a CLV-2534 Laser Vibrometer (Polytec, Germany).

132   The laser beam was focussed onto the incudostapedial joint, or the head of the stapes,

133   depending upon target angle and accessibility in individual preparations. No noticeable

134   difference between the two recording sites was observed. Care was taken throughout data

135   acquisition to maintain the highest reflected signal possible, by adjusting the focus of the

136   laser point to account for gross physiological movement within the preparation. The output

137   voltage from the vibrometer was band-pass filtered between 100 Hz – 100 kHz, with a

138   sensitivity of 2mm/s/V and a gain of x100.

139   Experimental control and data acquisition were performed using a PC with custom programs

140   written in MATLAB (MathWorks, MA). Data analysis was performed using Origin
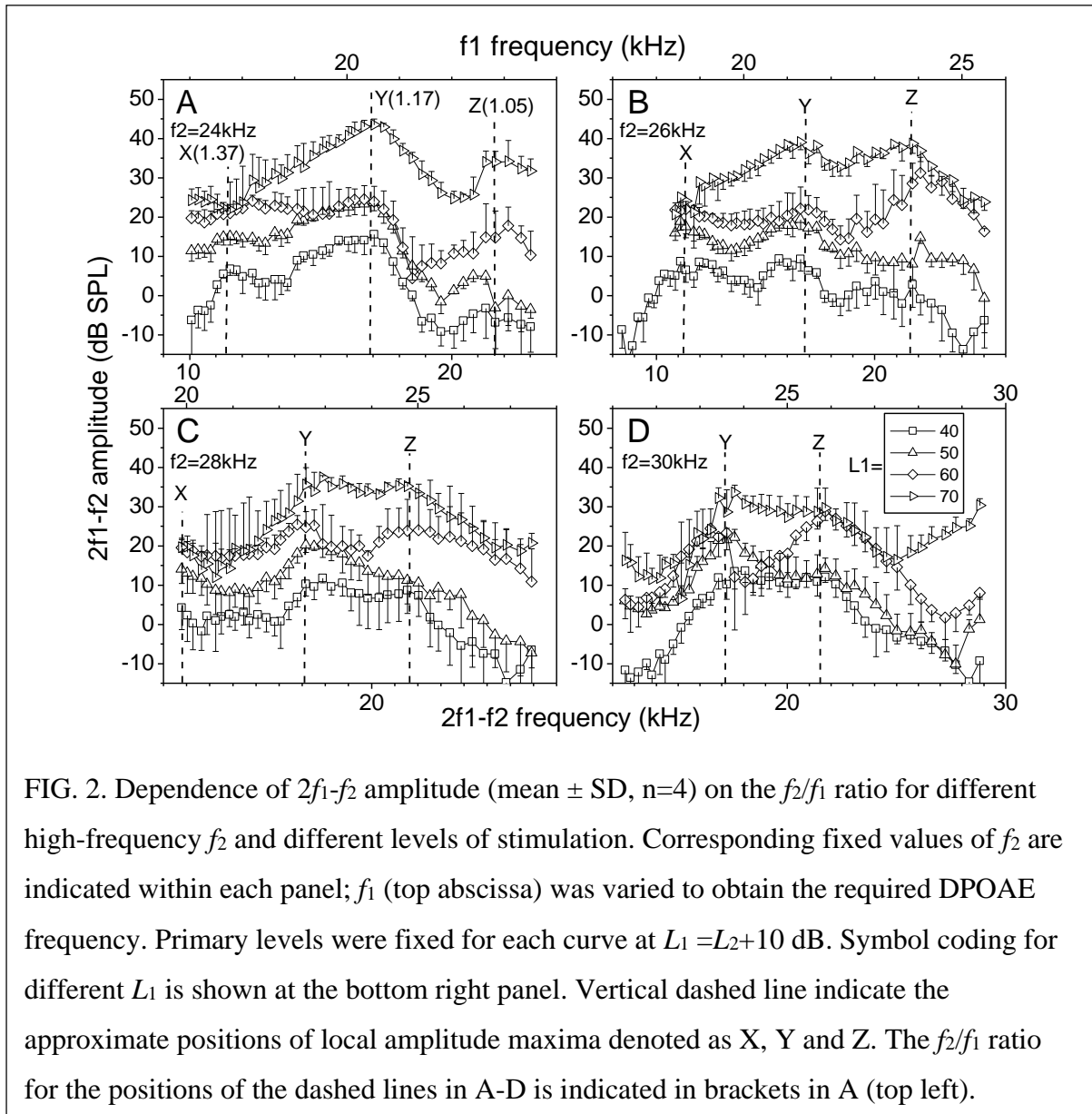
141 (OriginLab, MA). Acoustic and laser measurements were conducted in healthy cochleae, and

142 post mortem following overdose using Euthatal, in the presence of sodium salicylate crystals

143 placed onto the round window membrane.

III. RESULTS

145 The DPOAE amplitude as a function of primary frequency ratio has a well-known bell-like

146 shape (e.g. Brown *et al*., 1992) when constant f_2 is in the low-/mid-frequency range for

147 guinea pigs (Fig. 1). The maximum of this bell-like shape is observed at approximately the

148 same frequency for DPOAEs of different order (Fig. 1), where the order of DPOAE $mf_1 + nf_2$

149 is determined by the sum m+n. The position of this maximum is level dependent and it shifts

150 towards lower frequencies with increasing level of the primaries (Lukashkin and Russell,

151 2001; Lukashkin et al., 2007).

FIG. 1. Dependence of DPOAE amplitude on the f_2/f_1 ratio for low-frequency primaries in
a single preparation. Symbol coding for different DPOAEs is shown at the top panel. f_2
was fixed and its value is indicated within the panels; f_1 was varied to obtain the required
DPOAE frequency. Primary levels were fixed at $L_1 = L_2 + 10$ dB=40 dB SPL.

152

153 This dependence, however, becomes more complex for high-frequency primaries, namely

154 local amplitude maxima are superimposed onto the general bell-like shape when constant f_2 is

155 kept above 12 kHz (Lukashkin *et al.*, 2007). The local maxima generated for f_2 at and above

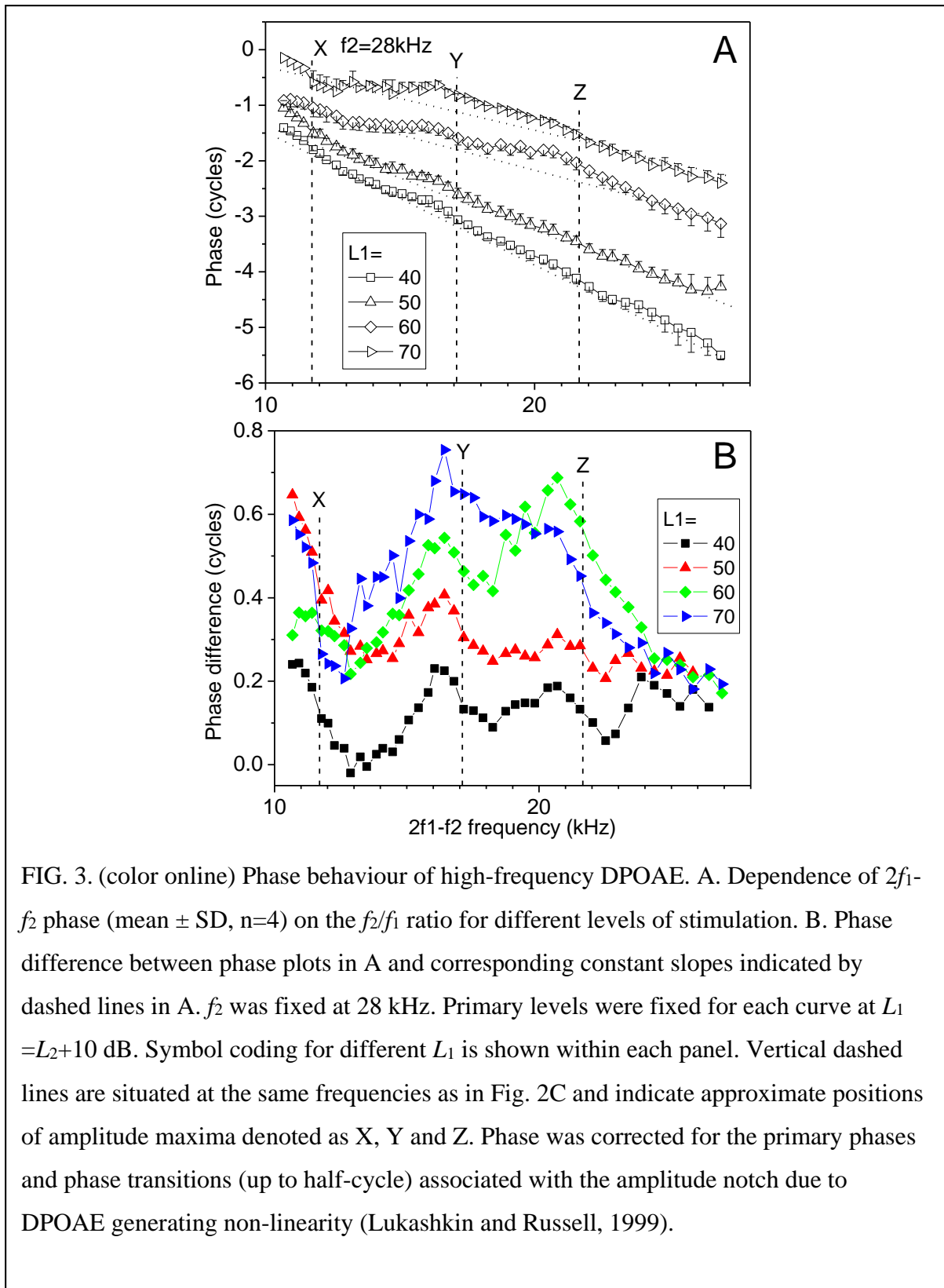156 24 kHz are marked as X, Y and Z in Figure 2.

FIG. 2. Dependence of $2f_1$-f_2 amplitude (mean ± SD, n=4) on the f_2/f_1 ratio for different high-frequency f_2 and different levels of stimulation. Corresponding fixed values of f_2 are indicated within each panel; f_1 (top abscissa) was varied to obtain the required DPOAE frequency. Primary levels were fixed for each curve at $L_1 = L_2 + 10$ dB. Symbol coding for different L_1 is shown at the bottom right panel. Vertical dashed line indicate the approximate positions of local amplitude maxima denoted as X, Y and Z. The f_2/f_1 ratio for the positions of the dashed lines in A-D is indicated in brackets in A (top left).

158 Regardless of f_2 value, the maxima remain at approximately the same frequency but, because

159 of presence of the general bell-like shape, their position may shift slightly for different

160 parameters of stimulation. These local amplitude maxima are separated by approximately

161 half-octave intervals. The maxima may not be pronounced at intermediate levels of the

162   primaries due to non-monotonic growth of the DPOAE amplitude (Lukashkin and Russell,

163   1999; Lukashkin et al., 2002), but they reappear at higher levels of the primaries. The phase

FIG. 3. (color online) Phase behaviour of high-frequency DPOAE. A. Dependence of $2f_1$-f_2 phase (mean ± SD, n=4) on the f_2/f_1 ratio for different levels of stimulation. B. Phase difference between phase plots in A and corresponding constant slopes indicated by dashed lines in A. f_2 was fixed at 28 kHz. Primary levels were fixed for each curve at L_1 =L_2+10 dB. Symbol coding for different L_1 is shown within each panel. Vertical dashed lines are situated at the same frequencies as in Fig. 2C and indicate approximate positions of amplitude maxima denoted as X, Y and Z. Phase was corrected for the primary phases and phase transitions (up to half-cycle) associated with the amplitude notch due to DPOAE generating non-linearity (Lukashkin and Russell, 1999).

164   of the high-frequency DPOAEs shows associated oscillations (illustrated for f_2=28 kHz in

Fig. 3) which occur with the same periodicity as the amplitude maxima. Similar phase

patterns are usually observed during wave interaction and may indicate the amplitude

maxima originate from the summation of waves at the DPOAE frequencies.

It is worth noting that the amplitude maxima are observed for the same DPOAE frequencies,

and, hence, for different primary ratios and different corresponding f_1, in both distortion

components ($2f_1$-f_2, $3f_1$-$2f_2$) analysed in this paper (Fig. 4). It has been observed previously

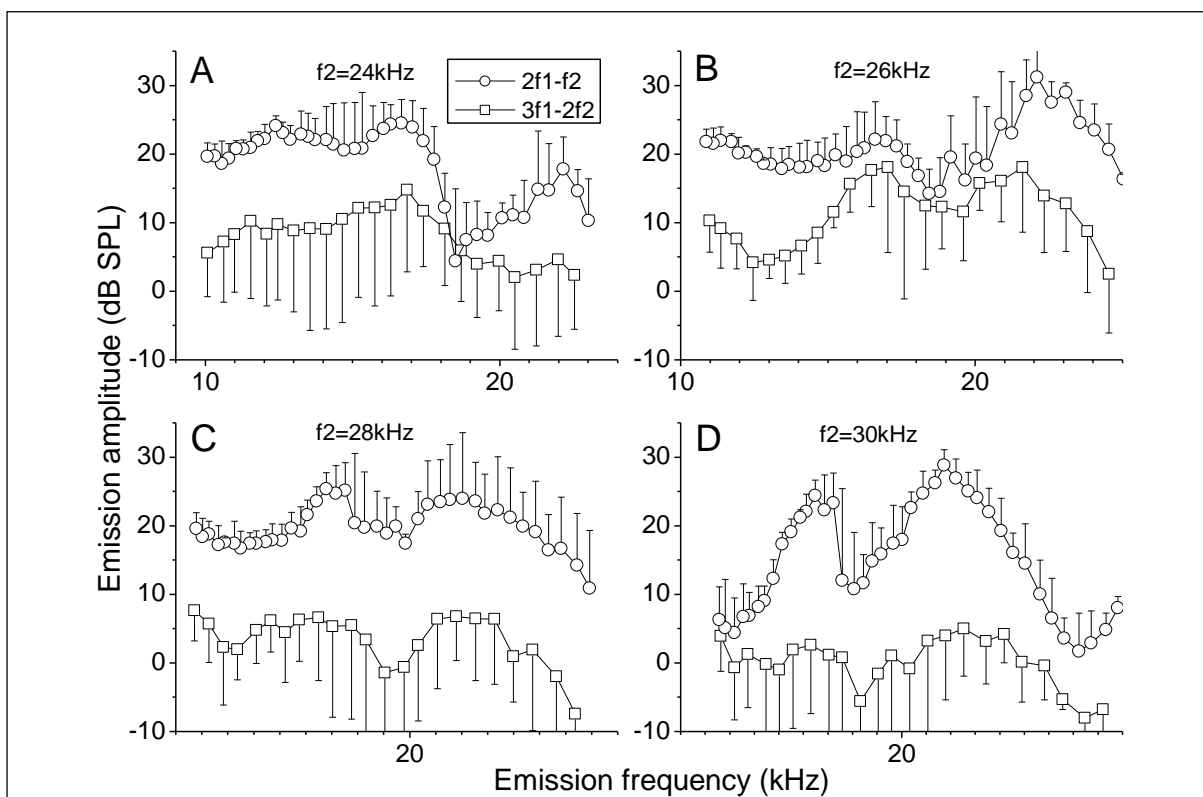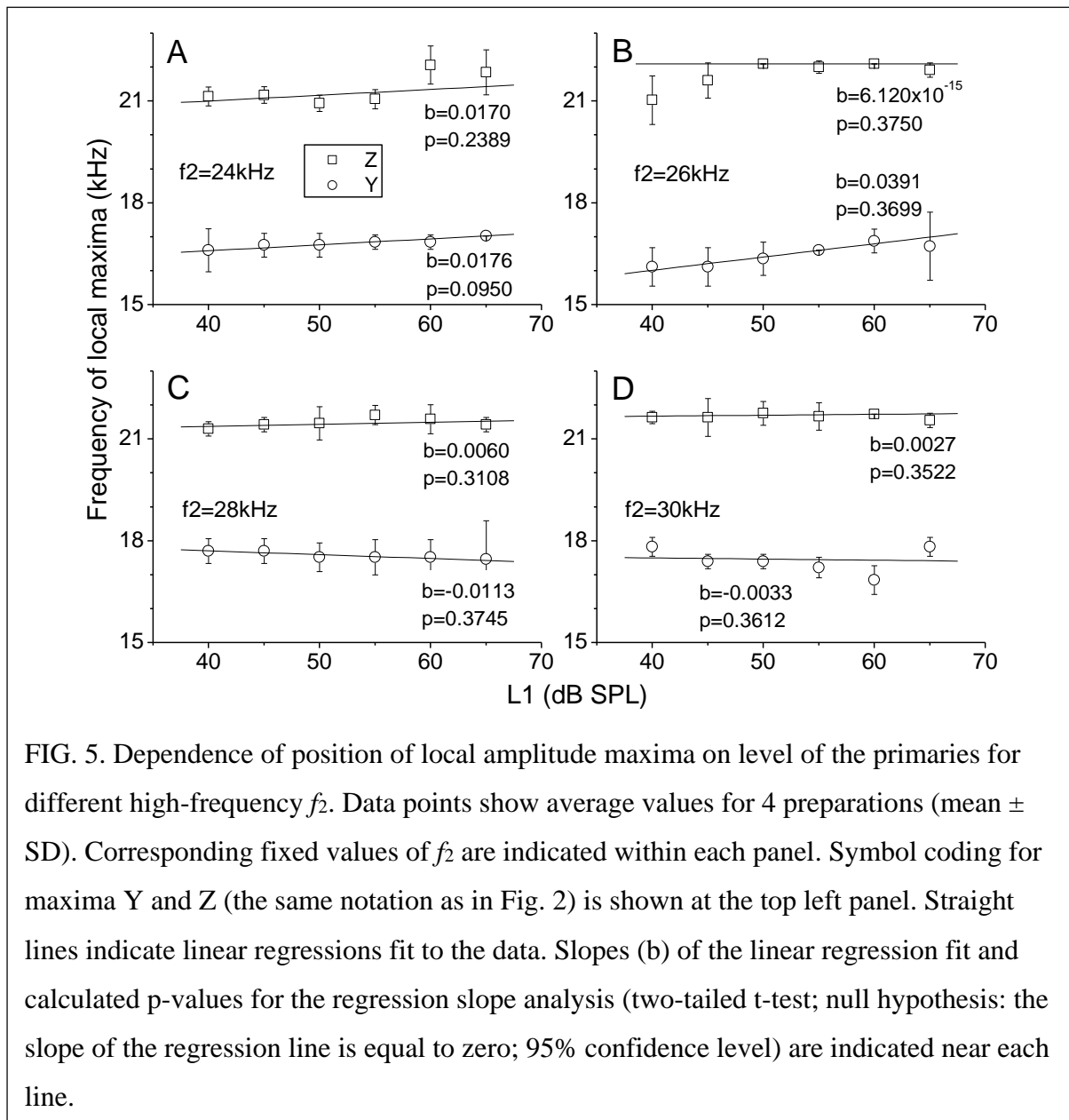that the $4f1$-$3f2$ emission contains these frequency specific maxima (Lukashkin *et al*. 2007).

FIG. 4. Dependence of DPOAE amplitude (mean ± SD, n=4) on the f_2/f_1 ratio for different high-frequency f_2. Corresponding fixed values of f_2 are indicated within each panel; f_1 was varied to obtain the required DPOAE frequency. Primary levels were fixed at $L_1 = L_2+10$ dB=50 dB SPL. Symbol coding for different orders of DPOAEs is shown in A.

For low levels of the primaries, the amplitude notches between the maxima are less

pronounced but the maxima are still visible. The maximum amplitude of the bell-like shape

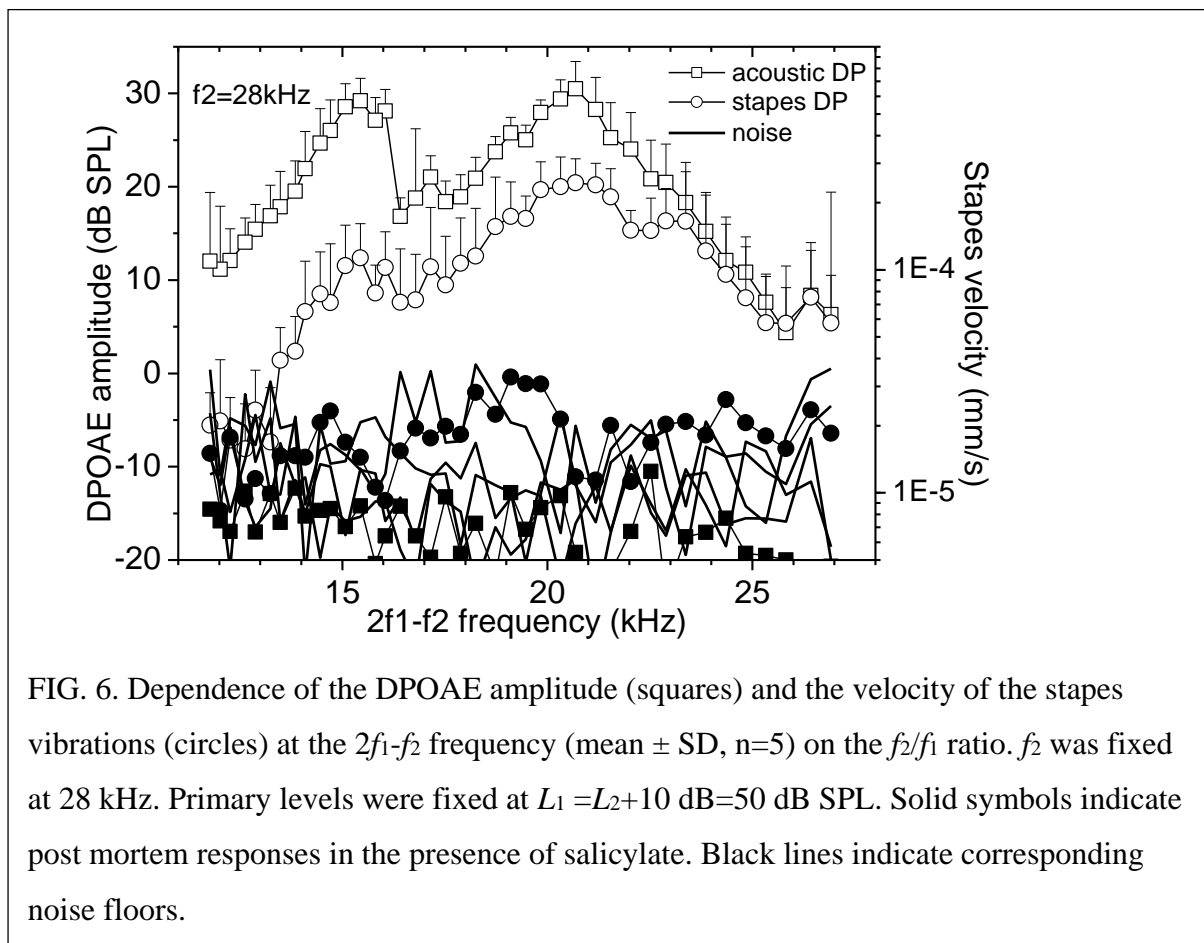of DPOAEs shifts to lower frequencies with increasing level of the primaries (e.g. see

176 Lukashkin and Russell, 2001; Lukashkin *et al*., 2007). There is, however, no statistically

177 significant (p = 0.05) shift in the frequency of the local amplitude maxima with increasing

178 level of the primaries (Fig. 5).

FIG. 5. Dependence of position of local amplitude maxima on level of the primaries for different high-frequency f_2. Data points show average values for 4 preparations (mean ± SD). Corresponding fixed values of f_2 are indicated within each panel. Symbol coding for maxima Y and Z (the same notation as in Fig. 2) is shown at the top left panel. Straight lines indicate linear regressions fit to the data. Slopes (b) of the linear regression fit and calculated p-values for the regression slope analysis (two-tailed t-test; null hypothesis: the slope of the regression line is equal to zero; 95% confidence level) are indicated near each line.

179

180 To confirm that the rippling pattern of the DPOAE amplitude is of cochlear origin, stapes

181 velocity at the $2f_1$-f_2 frequency in healthy and passive cochleae was recorded. Figure 6 shows

182 both the DPOAE amplitude and the velocity of the stapes vibrations at the $2f_1$-f_2 frequency in

183   healthy cochleae and post mortem in the presence of salicylate to block the residual OHC

184   somatic motility (Dieler *et al.*, 1991).

FIG. 6. Dependence of the DPOAE amplitude (squares) and the velocity of the stapes vibrations (circles) at the $2f_1$-f_2 frequency (mean ± SD, n=5) on the f_2/f_1 ratio. f_2 was fixed at 28 kHz. Primary levels were fixed at $L_1 = L_2 + 10$ dB = 50 dB SPL. Solid symbols indicate post mortem responses in the presence of salicylate. Black lines indicate corresponding noise floors.

185

186   The local maxima in the DPOAE amplitude and in the stapes distortion products were

187   conserved between the two measurement techniques. The low frequency maximum in the

188   stapes responses was relatively lower in amplitude than that recorded acoustically. This could

189   be due to multimodal vibrations of the stapes, whereby at low frequencies it moves in a

190   single, piston-like mode, but at higher frequencies displays complex rocking motion (e.g.

191   Eiber *et al.*, 2012). Because the stapes response was recorded in a single plane in our

192   experiments, summation of energy of these different modes at the level of the acoustic

193   response (DPOAE) in the ear canal could produce a relatively larger overall response. In post

194   mortem preparations where OHC somatic motility was additionally suppressed by salicylate,

195   both the DPOAE amplitude and the amplitude of distortion products of the stapes velocity

196   responses dropped into the noise floor. This indicates that the local maxima in the primary

197   ratio functions are of cochlea origin and physiologically vulnerable.

198   To examine whether the rippling pattern of the DPOAE amplitude was due to interaction

199   between emissions from the distortion source and the reflection source, a third, suppressor

200   tone which spanned a wide range of frequencies was added to the acoustic stimulation. When

201   the suppressor tone was added, it changed the dependence of the DPOAE amplitude on the

202   ratio of the primaries (Fig. 7).
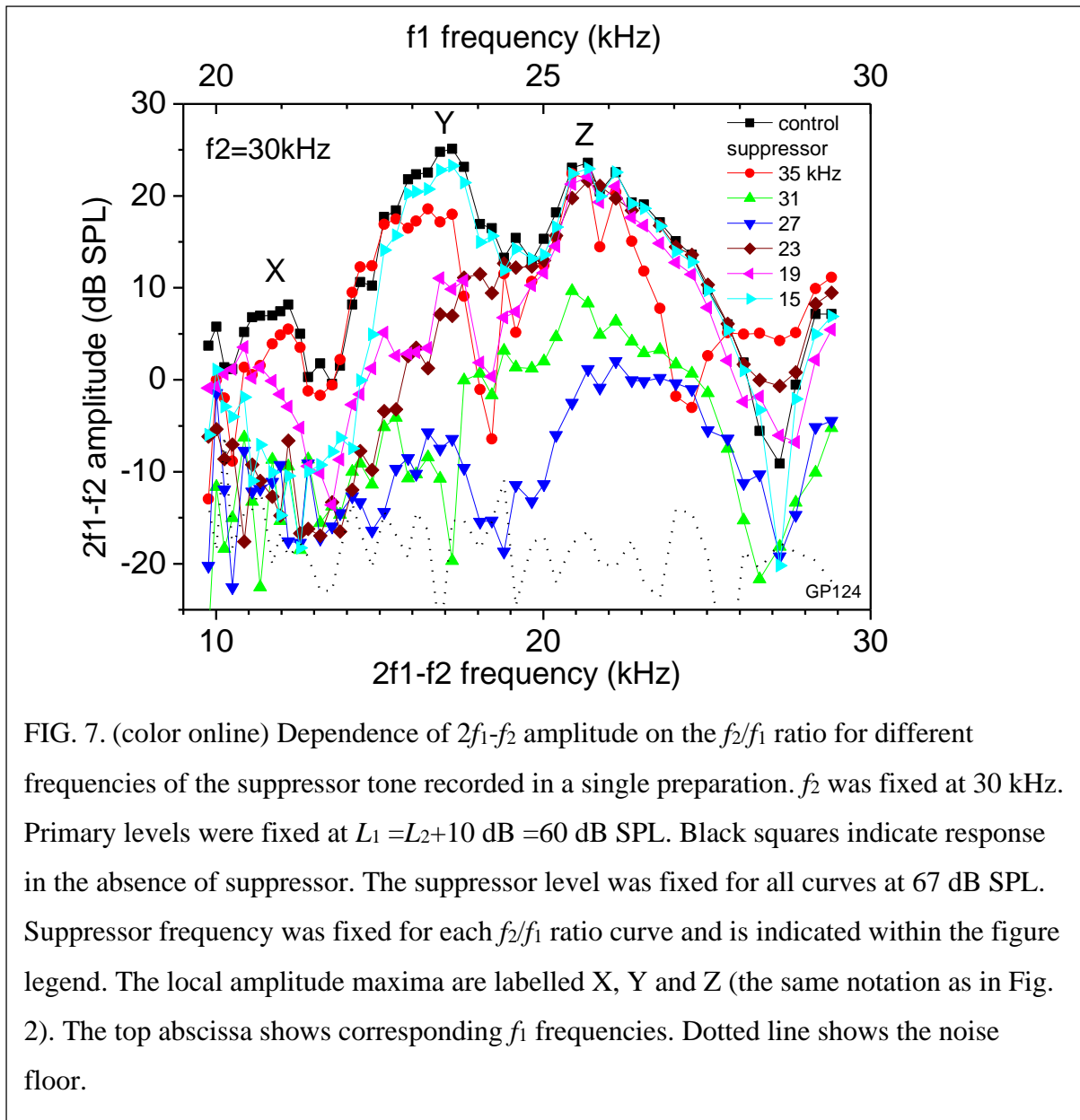
FIG. 7. (color online) Dependence of $2f_1$-f_2 amplitude on the f_2/f_1 ratio for different frequencies of the suppressor tone recorded in a single preparation. f_2 was fixed at 30 kHz. Primary levels were fixed at $L_1 = L_2 + 10$ dB $= 60$ dB SPL. Black squares indicate response in the absence of suppressor. The suppressor level was fixed for all curves at 67 dB SPL. Suppressor frequency was fixed for each f_2/f_1 ratio curve and is indicated within the figure legend. The local amplitude maxima are labelled X, Y and Z (the same notation as in Fig. 2). The top abscissa shows corresponding f_1 frequencies. Dotted line shows the noise floor.

Suppressor tones close to f_2 (27 and 31 kHz in Fig. 7) were the most efficient in decreasing the overall DPOAE amplitude over a wide frequency range. Presumably, because these suppressors effectively suppress responses of both primaries in the region of their overlap. For all frequencies of the suppressor, the absolute decrease of the DPOAE amplitude was, however, larger for the low-frequency shoulder of the ratio dependence and, hence, low-frequency maxima X and Y were suppressed more efficiently than maximum Z. Peak Z was reduced in the presence of the suppressor only when the suppressor frequency was close to f_2.

211   Maxima X and Y were also affected by suppressors close to the f_2, but there appeared to be

212   little evidence of a functional relationship between suppressor frequency and suppression

213   efficiency for lower frequencies. Whilst the observation that suppression is more efficient for

214   suppressor tones closer in frequency to f_2 is well supported (Brown and Kemp, 1984; Harris

215   *et al*., 1992; Kummer *et al*., 1995; Abdala *et al*., 1996; Martin *et al*., 1998), the finding that

216   the absolute decrease of the DPOAE amplitude was larger for the low-frequency shoulder of

217   the ratio dependence may be somewhat counterintuitive. This effect can be explained by

218   considering the responses of the primaries in the region of their overlap, which is close to the

219   f_2 place and is thought to be the region where energy at the distortion is originally produced

220   (Brown and Kemp, 1984). The low-frequency suppressor tone's effect (15 and 19 kHz

221   suppressor, Fig. 7) on the DPOAE amplitude would be relatively small for small f_2/f_1 ratios

222   when the primary frequencies are close to each other and produce large responses in the

223   overlap region. When primary frequency separation increases, the suppressor becomes

224   effective against f_1 when f_1 is further away from f_2 and when responses of the suppressor and

225   f_1 in the primary overlap region become comparable. Significantly for this study, there was no

226   local suppression effect observed for maxima X, Y and Z whilst the suppressor frequency

227   was close to the $2f_1$-f_2, hence, contribution of the secondary emission source into the

228   generation of the local amplitude maxima was minimal.

229   **IV. DISCUSSION**

230   This study investigates the origin of ripples in the amplitude of high-frequency DPOAEs

231   which form local amplitude maxima at specific DPOAE frequencies independent of the

232   primary frequencies and levels. The maxima are separated by approximately half octave

233   intervals and they are observed at the same frequencies in the DPOAEs of different order and,

234   in fact, in responses of the stapes at the distortion frequencies. A third high-level tone, while

235   suppressing overall amplitude of the DPOAE, does not suppress this rippling pattern whether

236   the suppressor frequency is close to f_1, f_2 or to the frequency of emission.

237   The rippling pattern is generated within the cochlea and is already seen in the stapes

238   vibrations at the corresponding frequencies. Logarithmic scaling of these frequencies

239   resembles the cochlear logarithmic scaling (von Békésy, 1960; Greenwood, 1990), which

240   makes it unlikely that the local maxima are artefacts of the acoustic systems used for DPOAE

241   stimulation and recording. The frequencies of the local maxima appear to be due to the

242   intrinsic characteristics of the guinea pig cochlea because these frequencies do not depend on

243   the primary frequencies. They are essentially the same for different f_2 frequencies and the

244   amplitude maxima appear at the same frequencies in higher order emissions, although this

245   means that they appear at very different primary ratios f_2/f_1.

246   It is unlikely that the rippling pattern is generated by the primary mechanisms responsible for

247   the DPOAE generation at the place of primary overlap near the f_2 CF place (Brown and

248   Kemp, 1984). Increase in the overlap of the primaries and shift of their excitation envelopes

249   to the base of the cochlea with increasing the level of stimulation causes a frequency shift, for

250   example, the DPOAE filter functions (Lukashkin and Russell, 2001; Lukashkin *et al*., 2007)

251   and the DPOAE fine structure (He and Schmiedt, 1993). The local amplitude maxima do not,

252   however, exhibit a level dependent frequency shift. The absence of this frequency shift, along

253   with the frequency invariance of the maxima relative to the f_2, implies that the maxima relate

254   to an amplitude modulation of DPOAE by phenomena related to cochlear structure. This is

255   because any characteristics of the DPOAE governed by mechanisms associated with

256   distortion generation should be strongly influenced by changes in the primary frequency or

257   by changing primary level.

258   On the other hand, phase of the high-frequency DPOAEs shows oscillations which occur with

259   the same periodicity as the amplitude maxima. Similar phase pattern is usually observed

260   during wave interaction and may indicate generation of the amplitude maxima due to

261   summation of waves at the DPOAE frequencies. In that case, what is the possible origin of

262   these waves? The independence of the local maxima on the frequency of the primary tones

263   makes it unlikely that these maxima are generated by multiple wave interference between

264   distortion-source and reflection-source emissions, which has been used to explain the

265   frequency periodicity of the evoked emissions recorded from the same species in other

266   experiments (Goodman *et al*., 2003; Withnell *et al*., 2003). An additional argument against

267   the local maxima being due to phase interference of emissions from different sources comes

268   from our suppression experiments. DPOAE fine structure has been shown to exist in rodents

269   (Withnell *et al*., 2003), although it presents a cyclic periodicity that is slower than in humans

270   (Talmadge *et al*., 1999, Kalluri and Shera, 2001). If the local maxima and minima were due

271   to a kind of fine structure specific to this species, then placement of the suppressor tone

272   adjacent to the $2f_1$-f_2 would abolish the peak and trough pattern seen in the DPOAE ratio

273   functions presented here. Such observations have been made in humans, where the

274   mechanism responsible for the generation of DPOAE fine structure is widely agreed upon

275   (Heitmann *et al*., 1998; Dhar and Shaffer, 2004). However, the $2f_1$-f_2 signals as a function of

276   the primary ratio described here still show the same peak and trough distribution, in the

277   presence of a suppressor. It therefore follows that the reflection source emissions from the

278    $2f_1$-f_2 CF place are not responsible for the observed local maxima.

279   Half an octave separation between the local maxima indicate that they may originate from

280   periodic interaction between the basilar membrane and tectorial membrane travelling waves.

281   It is thought that the tectorial membrane is tuned to a frequency about half an octave below

282   the frequency of its cochlea location (Allen, 1980; Gummer *et al*., 1996; Lukashkin *et al*.,

283   2010) and is capable of maintaining a local travelling wave (Ghaffari *et al.*, 2007; Jones *et*

284   *al.*, 2013). Evidence for the half-octave shift in the tectorial membrane tuning comes from

285   mechanical (Gummer *et al.*, 1996; Legan *et al.*, 2000; Lukashkin *et al.*, 2012), acoustic

286   (Allen and Fahey, 1993; Lukashkin and Russell, 2003; Lukashkin *et al.*, 2004, 2007) and

287   neural (Liberman, 1978; Allen and Fahey, 1993; Taberner and Liberman, 2005; Russell *et al.*,

288   2007) cochlear responses. The local DPOAE amplitude maxima observed here may relate to

289   this difference in tuning of the basilar and tectorial membranes. Interactions between

290   travelling waves on the tectorial and basilar membranes is, however, a local phenomenon

291   and, hence, should be affected by changes in the f_2 frequency. The local amplitude maxima

292   described here are independent of the primary frequencies and are a global phenomenon

293   associated with propagation rather than generation of energy at the DPOAE frequencies.

294   Therefore, it is unlikely that the tectorial membrane – basilar membrane wave interaction

295   contributes to the generation of the rippling pattern.

296   Instead, the DPOAE amplitude ripples described here may reflect the formation of standing

297   waves in the cochlea due to multiple internal reflections due to the impedance mismatch at

298   the middle ear boundary (Shera and Zweig, 1991; Russell and Kössl, 1999; Shera, 2003).

299   This multiple wave reflection and interference have been suggested to contribute to

300   generation of DPOAEs (Stover *et al.*, 1996; Withnell *et al.*, 2003; Dhar and Shaffer, 2004),

301   transient evoked otoacoustic emissions (e.g. Kemp, 1978), stimulus frequency otoacoustic

302   emission (Goodman *et al.*, 2003; Berezina-Greene and Guinan, 2015), spontaneous

303   otoacoustic emissions (SOAE) (Kemp, 1979; Russell and Kössl, 1999; Shera, 2003), rippling

304   pattern in basilar membrane responses (Shera and Cooper, 2013) and microstructure in

305   hearing threshold measurements (Shera, 2015). A recent study exploring the suppression

306   pattern of SOAEs in humans (Manley and van Dijk, 2016) found a secondary lobe of

307   suppression located half an octave above the SOAE CF in addition to a V-shaped suppression

308   region around the CF. It was suggested that the changes in suppression efficacy seen at these

309   points could be due to the suppressor tone nearing nodes and anti-nodes of the SOAE

310   standing wave. The finding reported here that the distance between maxima X, Y and Z is

311   close to half an octave would appear to support the hypothesis that the ripple in the $2f_1$-f_2

312   amplitude is due to modulation by the SOAE standing wave. The formation of the rippling

313   pattern reported here is due to multiple internal reflections with two provisos. The first is that

314   reflected waves propagate in a linear passive regime. The second is that the boundary

315   conditions, which enable these reflections, do not depend on the non-linear active process.

316   The rippling pattern should then, as we have observed, be independent of stimulus

317   parameters. Within this framework, the rippling is present only in the amplitude and phase of

318   high-frequency DPOAEs because this is favourable for the formation of standing waves. Net

319   energy losses during the round-trip for reflected travelling waves produced by low-frequency

320   primaries, which peak at the cochlear apex, may be too high to support the formation of the

321   standing waves.

322   SOAEs, which are thought to be produced due to the formation of the standing waves (Kemp,

323   1979; Russell and Kössl, 1999; Shera, 2003), are far more prominent in humans than in

324   guinea pigs due to the less regular geometry of the primate cochlea (Kemp, 1986; Lonsbury-

325   Martin *et al*., 1988; Shera and Guinan, 1999). Very few examples of independently measured

326   SOAEs in anaesthetised guinea pig exist (Brown *et al*., 1990; Ohyama *et al*., 1991; Nuttall *et*

327   *al*., 2004). The observation that the frequencies of the local amplitude maxima of DPOAEs

328   are conserved across animals in our experiments may also be due to high levels of anatomical

329   consistency between experimental subjects. The boundary conditions governing formation of

330   the standing waves in guinea pig cochleae could be far less variable, as rodent cochleae are

331   structurally more ordered.

332   That the presence of standing waves in the rodent cochlea is only suggested by their

333   modulation of the small DPOAE signal is unsurprising. Morphologically regular rodent

334   cochleae do not normally allow generation and emission of high-frequency SOAEs. As a

335   result, these standing waves remain visible only by their interaction with, and influence on

336   DPOAE amplitudes at specific frequencies.

337   It is worth noting that the DPOAE generation sites are discussed as point sources here and

338   actual generation of the distortion products may occur over an extended region along the

339   cochlea. Hence, it is possible that this extended region can somehow contribute to formation

340   of the rippling pattern of the DPOAE amplitude observed for the high frequency primaries.

341   Regions of interaction between extended source areas should not, however, confound our

342   conclusions.

343   **CONCLUSION**

344   The rippling pattern of high-frequency DPOAE amplitude and corresponding phase

345   oscillations is of cochlear origin and is a global phenomenon associated with propagation

346   rather than generation of energy at the DPOAE frequencies. Frequencies of the local

347   amplitude maxima of the rippling pattern do not depend on parameters of stimulation (i.e.

348   frequency and level of the primaries). The rippling pattern is not suppressed by a third, high-

349   level tone and is likely to originate from multiple internal reflections and formation of

350   standing waves at the DPOAE frequencies within the cochlea.

355   **REFERENCES**

356 Abdala, C., Sininger, Y. S., Ekelid, M., and Zeng, F-G. (**1996**). ''Distortion product

357 otoacoustic emission suppression tuning curves in human adults and neonates,'' Hear. Res.

358 **98**, 38–53. (DOI:10.1016/0378-5955(96)00056-1)

359 Allen, J.B. (**1980**). "Cochlear micromechanics – A physical model of transduction," J.

360 Acoust. Soc. Am. **68**, 1660–1670. (DOI:10.1121/1.385198)

361 Allen, J. B., and Fahey, P. F. (**1993**). "A second cochlear-frequency map that correlates

362 distortion product and neural tuning measurements," J. Acoust. Soc. Am. **94**, 809–816.

363 (DOI:10.1121/1.408182)

364 Avan, P., Büki, B., and Petit, C. (**2013**). "Auditory distortions: origins and functions,"

365 Physiol. Rev. **93**, 1563-1619. (DOI:10.1152/physrev.00029.2012)

366 Békésy, G. von (**1960**). *Experiments in Hearing* (McGraw-Hill, New York).

367 Berezina-Greene, M. A., and Guinan, J. J. (**2015**). "Stimulus frequency otoacoustic emission

368 delays and generating mechanisms in guinea pigs, chinchillas, and simulations," J. Assoc.

369 Res. Otolaryngol. **16**, 679-694. (DOI:10.1007/s10162-015-0543-7)

370 de Boer, E., Nuttall, A. L., and Shera, C. A. (**2007**). "Wave propagation patterns in a

371 "classical" three-dimensional model of the cochlea," J. Acoust. Soc. Am. **121**, 352-362.

372 (DOI:10.1121/1.2385068)

373 Brown, A. M., Gaskill, S. A., and Williams, D. M. (**1992**). "Mechanical filtering of sound in

374 the inner ear," Proc. R. Soc. B. **250**, 29-34. (DOI:10.1098/rspb.1992.0126)

375 Brown, A. M., Harris, F. P., and Beveridge, H. A. (**1996**). "Two sources of acoustic distortion

376 products from the human cochlea," J. Acoust. Soc. Am. **100**, 3260-3267.

377 (DOI:10.1121/1.417209)

378 Brown, A. M., and Kemp, D. T. (**1984**). "Suppressibility of the $2f_1$-f_2 stimulated acoustic

379 emissions in gerbil and man," Hear. Res. **13**, 29-37. (DOI:10.1016/0378-5955(84)90092-3)

380 Brown, A. M., Woodward, S., and Gaskill, S. A. (**1990**). "Frequency variation in spontaneous

381 sound emissions from guinea pig and human ears," Eur. Arch. Otorhinolaryngol. **247**, 24-28.

382 (DOI:10.1007/BF00240944)

383 Dhar, S., and Shaffer, L. A. (**2004**). "Effects of a suppressor tone on distortion product

384 otoacoustic emissions fine structure: Why a universal suppressor level is not a practical

385 solution to obtaining single-generator DP-grams," Ear Hear. **25**, 573-585.

386 Dieler, R., Shehata-Dieler, W. E., and Brownell, W. E. (**1991**). "Concomitant salicylate-

387 induced alterations of outer hair cell subsurface cisternae and electromotility," J. Neurocytol.

388 **20**, 637– 653. (DOI:10.1007/BF01187066)

389 Eiber, A., Huber, A. M., Lauxmann, M., Chatzimichalis, M., Sequeira, D., and Sim, J. H.

390 (**2012**). "Contribution of complex stapes motion to cochlea activation," Hear. Res. **284**, 82-

391 92. (DOI:10.1016/j.heares.2011.11.008)

392 Ghaffari, R., Aranyosi, A. J., and Freeman, D. M. (**2007**). "Longitudinally propagating

393 traveling waves of the mammalian tectorial membrane," Proc. Natl. Acad. Sci. USA **104**,

394 16510-16515. (DOI:10.1073/pnas.0703665104)

395 Goodman, S. S., Withnell, R. H., and Shera, C. A. (**2003**). "The origin of SFOAE

396 microstructure in the guinea pig," Hear. Res. **183**, 7-17. (DOI: 10.1016/S0378-

397 5955(03)00193-X)

398 Greenwood, D. D. (**1990**). "A cochlear frequency-position function for several species—29

399 years later," J. Acoust. Soc. Am. **87**, 2592-2605. (DOI:10.1121/1.399052)

400   Gummer, A. W., Hemmert, W., and Zenner, H. P. (**1996**). "Resonant tectorial membrane

401   motion in the inner ear: its crucial role in frequency tuning," Proc. Natl. Acad. Sci. USA **93**,

402   8727–8732.

403   Harris, F. P., Probst, R., and Xu, L. (**1992**). ''Suppression of the $2f_1$-f_2 otoacoustic emission in

404   humans,'' Hear. Res. **64**, 133–141. (DOI:10.1016/0378-5955(92)90175-M)

405   He, N. J., and Schmiedt, R. A. (**1993**). "Fine structure of the $2f_1$-f_2 acoustic distortion product:

406   Changes with primary level," J. Acoust. Soc. Am. **94**, 2659-2669. (DOI:10.1121/1.407350)

407   Heitmann, J., Waldmann, B., Schnitzler, H.-U., Plinkert, P. K., and Zenner, H. P. (**1998**).

408   "Suppression of distortion product otoacoustic emissions (DPOAE) near $2f1- f2$ removes

409   DP-gram fine structure—Evidence for a secondary generator," J. Acoust. Soc. Am. **103**,

410   1527-1531. (DOI:10.1121/1.421290)

411   Hilger, A. W., Furness, D. N., and Wilson, J. P. (**1995**). "The possible relationship between

412   transient evoked otoacoustic emissions and organ of Corti irregularities in the guinea pig,"

413   Hear. Res. **84**, 1-11. (DOI:10.1016/0378-5955(95)00007-Q)

414   Jones, G. P., Lukashkina, V. A., Russell, I. J., Elliott, S. J., and Lukashkin, A. N. (**2013**).

415   "Frequency-dependent properties of the tectorial membrane facilitate energy transmission

416   and amplification in the cochlea," Biophys. J. **104**, 1357-1366.

417   (DOI:10.1016/j.bpj.2013.02.002)

418   Kalluri, R. and Shera, C. A. (**2001**). "Distortion-product source unmixing: A test of the two-

419   mechanism model for DPOAE generation," J. Acoust. Soc. Am. **109**, 622-637.

420   (DOI:10.1121/1.1334597)

421   Kemp, D. T. (**1978**). "Stimulated acoustic emissions from within the human auditory

422   system," J. Acoust. Soc. Am. **64**, 1386-1391. (DOI:10.1121/1.382104)

423   Kemp, D. T. (**1979**). "Evidence of mechanical nonlinearity and frequency selective wave

424   amplification in the cochlea," Arch. Otorhinolaryngol. **224**, 37-45.

425   (DOI:10.1007/BF00455222)

426   Kemp, D. T. (**1986**). "Otoacoustic emissions, travelling waves and cochlear mechanisms,"

427   Hear. Res. **22**, 95-104. (DOI:10.1016/0378-5955(86)90087-0)

428   Kemp, D. T., and Brown, A. M. (**1983**). "An integrated view of cochlear mechanical

429   nonlinearities observable from the ear canal," in *Mechanics of Hearing*, edited by E. de Boer,

430   and M. A. Viergever (Springer, Netherlands), pp. 75-82. (DOI: 10.1007/978-94-009-6911-

431   7_9)

432   Knight, R. D., and Kemp, D. T. (**2000**). "Indications of different distortion product

433   otoacoustic emission mechanisms from a detailed f_1, f_2 area study," J. Acoust. Soc. Am. **107**,

434   457-473. (DOI:10.1121/1.428351)

435   Konrad-Martin, D., Neely, S. T., Keefe, D. H., Dorn, P. A., and Gorga, M. P. (**2001**).

436   "Sources of distortion product otoacoustic emissions revealed by suppression experiments

437   and inverse fast Fourier transforms in normal ears," J. Acoust. Soc. Am. **109**, 2862-2879.

438   (DOI:10.1121/1.1370356)

439   Kummer, P., Janssen, T., and Arnold, W. (**1995**). ''Suppression tuning characteristics of the

440    $2f_1$-f_2 distortion-product emissions in humans,'' J. Acoust. Soc. Am. **98**, 197–210.

441   (DOI:10.1121/1.413747)

442   Legan, P. K., Lukashkina, V. A., Goodyear, R. J., Kössl, M., Russell, I. J., and Richardson,

443   G. P. (**2000**). "A targeted deletion in α-tectorin reveals that the tectorial membrane is required

444   for the gain and timing of cochlear feedback," Neuron **28**, 273-285. (DOI:10.1016/S0896-

445   6273(00)00102-1)

446 Liberman, M. C. (**1978**). "Auditory-nerve response from cats raised in a low-noise chamber,"

447 J. Acoust. Soc. Am. **63**, 442–455. (DOI:10.1121/1.381736)

448 Lonsbury-Martin, B. L., Martin, G. K., Probst, R., and Coats, A. C. (**1988**). "Spontaneous

449 otoacoustic emissions in a nonhuman primate. II. Cochlear anatomy," Hear. Res. **33**, 69-93.

450 (DOI:10.1016/0378-5955(88)90021-4)

451 Lukashkin, A. N., Legan, P. K., Weddell, T. D., Lukashkina, V. A., Goodyear, R. J.,

452 Welstead, L., Petit, C., Russell, I. J., and Richardson, G. P. (**2012**). "A mouse model for

453 human deafness DFNB22 reveals that hearing impairment is due to a loss of inner hair cell

454 stimulation," Proc. Natl. Acad. Sci. USA **109**, 19351–19356.

455 (DOI:10.1073/pnas.1210159109)

456 Lukashkin, A. N., Lukashkina, V. A., Legan, P. K., Richardson, G. P., and Russell, I. J.

457 (**2004**). "Role of the tectorial membrane revealed by otoacoustic emissions recorded from

458 wild-type and transgenic *Tecta$^{\Delta ENT/\Delta ENT}$* mice," J. Neurophysiol. **91**, 163-171.

459 (DOI:10.1152/jn.00680.2003)

460 Lukashkin, A. N., Lukashkina, V. A., and Russell, I. J. (**2002**). "One source for distortion

461 product otoacoustic emissions generated by low-and high-level primaries," J. Acoust. Soc.

462 Am. **111**, 2740-2748. (DOI:10.1121/1.1479151)

463 Lukashkin, A. N., Richardson, G. P., and Russell, I. J. (**2010**). "Multiple roles for the tectorial

464 membrane in the active cochlea," Hear. Res. **266**, 26-35. (DOI:10.1016/j.heares.2009.10.005)

465 Lukashkin, A. N., and Russell, I. J. (**1999**). "Analysis of the $f2-f1$ and $2f1-f2$ distortion

466 components generated by the hair cell mechanoelectrical transducer: Dependence on the

467 amplitudes of the primaries and feedback gain," J. Acoust. Soc. Am. **106**, 2661-2668.

468 (DOI:10.1121/1.428096)

469   Lukashkin, A. N., and Russell, I. J. (**2001**). "Origin of the bell-like dependence of the

470   DPOAE amplitude on primary frequency ratio," J. Acoust. Soc. Am. **110**, 3097-3106.

471   (DOI:10.1121/1.1417525)

472   Lukashkin, A. N., and Russell, I. J. (**2003**). "A second, low frequency mode of vibration in

473   the intact mammalian cochlea," J. Acoust. Soc. Am. **113**, 1544-1550.

474   (DOI:10.1121/1.1535941)

475   Lukashkin, A. N., Smith, J. K., and Russell, I. J. (**2007**). "Properties of distortion product

476   otoacoustic emissions and neural suppression tuning curves attributable to the tectorial

477   membrane resonance," J. Acoust. Soc. Am. **121**, 337-343. (DOI:10.1121/1.2390670)

478   Manley, G. A., and van Dijk, P. (**2016**). "Frequency selectivity of the human cochlea:

479   Suppression tuning of spontaneous otoacoustic emissions," Hear. Res. **336**, 53-62.

480   (DOI:10.1016/j.heares.2016.04.004)

481   Martin, G. K., Jassir, D., Stagner, B. B., Whitehead, M. L., and Lonsbury-Martin, B. L.

482   (**1998**). "Locus of generation for the 2f1− f2 vs 2f2− f1 distortion-product otoacoustic

483   emissions in normal-hearing humans revealed by suppression tuning, onset latencies, and

484   amplitude correlations," J. Acoust. Soc. Am. **103**, 1957-1971. (DOI:10.1121/1.421347)

485   Nuttall, A. L., Grosh, K., Zheng, J., De Boer, E., Zou, Y., and Ren, T. (**2004**). "Spontaneous

486   basilar membrane oscillation and otoacoustic emission at 15 kHz in a guinea pig," J. Assoc.

487   Res. Otolaryngol. **5**, 337-348. (DOI:10.1007/s10162-004-4045-2)

488   Ohyama, K., Wada, H., Kobayashi, T., and Takasaka, T. (**1991**). "Spontaneous otoacoustic

489   emissions in the guinea pig," Hear. Res. **56**, 111-121. (DOI:10.1016/0378-5955(91)90160-B)

490   Russell, I. J., and Kössl, M. (**1999**). "Micromechanical responses to tones in the auditory

491   fovea of the greater mustached bat's cochlea," J. Neurophysiol. **82**, 676-686.

492   Russell, I. J., Legan, P. K., Lukashkina, V. A., Lukashkin, A. N., Goodyear, R. J., and

493   Richardson, G. P. (**2007**). "Sharpened cochlear tuning in a mouse with a genetically modified

494   tectorial membrane," Nat. Neurosci. **10**, 215-223. (DOI:10.1038/nn1828)

495   Russell, I. J., and Nilsen, K. E. (**1997**). "The location of the cochlear amplifier: Spatial

496   representation of a single tone on the guinea pig basilar membrane," Proc. Natl. Acad. Sci.

497   USA **94**, 2660-2664.

498   Shera, C. A. (**2003**). "Mammalian spontaneous otoacoustic emissions are amplitude-

499   stabilized cochlear standing waves," J. Acoust. Soc. Am. **114**, 244-262.

500   (DOI:10.1121/1.1575750)

501   Shera, C. A. (**2015**). "The spiral staircase: tonotopic microstructure and cochlear tuning," J.

502   Neurosci. **35**, 4683-4690. (DOI:10.1523/JNEUROSCI.4788-14.2015)

503   Shera, C. A., and Cooper, N. P. (**2013**). "Basilar-membrane interference patterns from

504   multiple internal reflection of cochlear traveling waves," J. Acoust. Soc. Am. **133**, 2224-

505   2239. (DOI:10.1121/1.4792129)

506   Shera, C. A., and Guinan, J. J. (**1999**). "Evoked otoacoustic emissions arise by two

507   fundamentally different mechanisms: A taxonomy for mammalian OAEs," J. Acoust. Soc.

508   Am. **105**, 782-798. (DOI:10.1121/1.426948)

509   Shera, C.A., and Zweig, G. (**1991**). "Reflection of retrograde waves within the cochlea and at

510   the stapes," J. Acoust. Soc. Am. **89**, 1290-1305. (DOI:10.1121/1.400654)

511   Stover, L. J., Neely, S. T., and Gorga, M. P. (**1996**). "Latency and multiple sources of

512   distortion product otoacoustic emissions," J. Acoust. Soc. Am. **99**, 1016-1024.

513   (DOI:10.1121/1.414630)

514   Taberner, A. M., and Liberman, M. C. (**2005**). "Response properties of single auditory nerve

515   fibers in the mouse," J. Neurophysiol. **93**, 557–569. (DOI:10.1152/jn.00574.2004)

516   Talmadge, C. L., Long, G. R., Tubis, A., and Dhar, S. (**1999**). "Experimental confirmation of

517   the two-source interference model for the fine structure of distortion product otoacoustic

518   emissions," J. Acoust. Soc. Am. **105**, 275-292. (DOI:10.1121/1.424584)

519   Vetešník, A., and Gummer, A. W. (**2012**). "Transmission of cochlear distortion products as

520   slow waves: A comparison of experimental and model data," J. Acoust. Soc. Am. **131**, 3914-

521   3934. (DOI:10.1121/1.3699207)

522   Withnell, R. H., Shaffer, L. A., and Talmadge, C. L. (**2003**). "Generation of DPOAEs in the

523   guinea pig," Hear. Res. **178**, 106-117. (DOI:10.1016/S0378-5955(03)00064-9)

524   Zweig, G., and Shera, C. A. (**1995**). "The origin of periodicity in the spectrum of evoked

525   otoacoustic emissions," J. Acoust. Soc. Am. **98**, 2018-2047. (DOI:10.1121/1.413320)